A Polygon-based Line Integral Method for Calculating Vorticity, Divergence, and Deformation from Non-uniform Observations

CHARLES N. HELMS * AND ROBERT E. HART

Florida State University, Tallahassee, Florida

1. Introduction

Traditional observational analyses of vorticity, divergence, and deformation fields usually rely on interpolating observations to either a Cartesian or spherical grid and then evaluating the appropriate finite difference equations. While this approach has the benefit of creating a set of gridded data which is easily processed via computer, it has been shown that greater accuracy can be obtained by using a line integration method, which employs Green's Theorem, on triangular regions (Spencer and Doswell 2001).

Bourassa and Ford (2010) implemented Green's Theorem using polygonal regions on gridded Quikscat wind data to calculated vorticity. Using this approach they demonstrated that regions defined by polygons of higher order can significantly reduce the uncertainty in vorticity calculations. At minimum, this approach requires some prior knowledge of the distribution of observations and it is preferable that the observations occur on a grid. Although this limitation prevents the use of this approach with observations which are not taken in a uniform pattern (e.g. dropsondes), their conclusion, that increasing the order of the bounding polygon decreases the uncertainty of the calculation, remains valid.

Accordingly, the present study describes a line integration method using polygonal regions which can be applied in situations where data is not distributed according to a predictable pattern. Section 2 briefly explains the application of Green's Theorem for calculating spatial derivatives. Details on the construction of the polygonal regions are provided in section 3. Section 4 provides a detailed evaluation of the accuracy of this approach and some concluding remarks are given in section 5.

---

* Corresponding author address: Charles N. Helms, Dept. of Earth, Ocean, and Atmospheric Sciences, Florida State University, Tallahassee, Florida 32306-4520
E-mail: chip.helms@gmail.com

2. Calculation of Spatial Derivatives

Spatial derivatives, such as vorticity, can be calculated using Green's Theorem on any given region whose bounding polygon is defined by three or more observations. More specifically, for a region bounded by the circuit C and having area A,

$$
\begin{aligned}
\frac{\partial Q}{\partial x} - \frac{\partial P}{\partial y} &= \frac{\oint_C P\mathrm{d}x + Q\mathrm{d}y}{A} \\
&\approx \frac{\sum(P\Delta x + Q\Delta y)}{A},
\end{aligned}
\tag{1}
$$

where Q and P are arbitrary variables and Δx and Δy are the zonal and meridional components of the edge lengths, respectively. By assigning the proper variables and signs to Q and P in Eq. (1) any spatial derivative can be calculated. Table 1 provides the appropriate values and resulting equations for vorticity, divergence, and deformation.

Variable	P	Q	Equation
Vorticity	u	v	$\frac{\partial v}{\partial x} - \frac{\partial u}{\partial y} \approx \frac{\sum(u\Delta x + v\Delta y)}{A}$
Divergence	$-v$	u	$\frac{\partial u}{\partial x} + \frac{\partial v}{\partial y} \approx \frac{\sum(u\Delta y - v\Delta x)}{A}$
Shearing Deformation	$-u$	v	$\frac{\partial v}{\partial x} + \frac{\partial u}{\partial y} \approx \frac{\sum(v\Delta y - u\Delta x)}{A}$
Stretching Deformation	v	u	$\frac{\partial u}{\partial x} - \frac{\partial v}{\partial y} \approx \frac{\sum(v\Delta x + u\Delta y)}{A}$

TABLE 1. Approximations of spatial derivative equations for vorticity, divergence, and deformation where u and v are the zonal and meridional components of the wind, respectively.
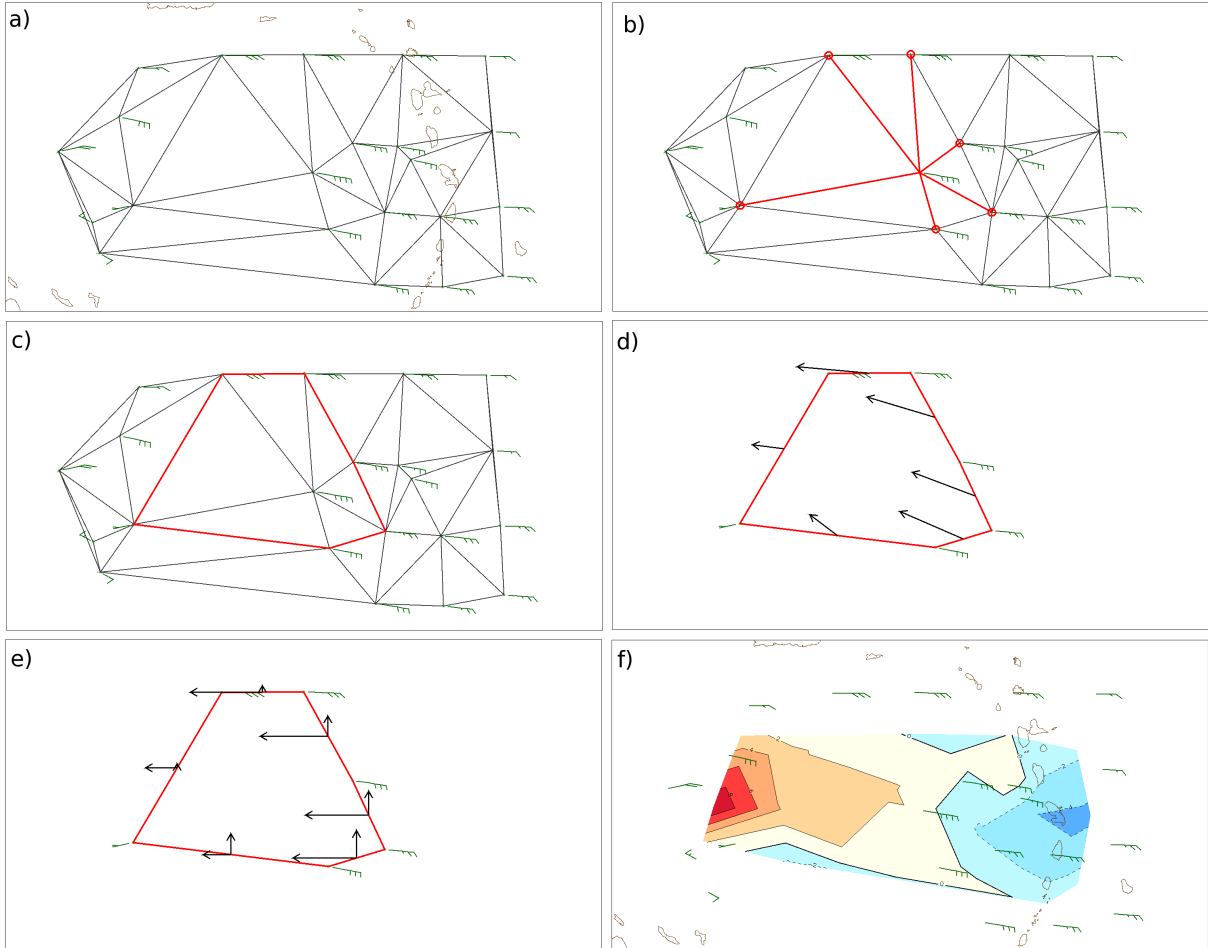
FIG. 1. Outline of the polygon construction process using data from the PREDICT field experiment (Montgomery et al. 2011). First, (a) a Delauney triangulation is constructed on the set of observations. (b) For each observation, the neighborhood of that observation (red highlighting) is found. (c) A polygon is then constructed using the neighborhood vertices. (d) The average wind vector for each edge is then calculated and then (e) decomposed. Applying Green's Theorem to calculate vorticity (see equation in Table 1) and repeating the process for each observation results in (f) a vorticity field.

3. Polygonal Region Construction

The polygon-based regions used in the method proposed here are an extension of the triangular regions used by previous methods (e.g. Spencer and Doswell 2001) and are constructed using a triangle tessellation. More specifically, a Delauney triangle tessellation is used due to a number of beneficial properties. Of greatest convenience to scientific study is the property that the Delauney triangulation on any given set of points is unique allowing for easy reproduction of results. Additionally, this type of triangulation maximizes the minimum of the three angles of each triangle meaning that the greatest number of triangles will be regular, or approach being regular. The benefit of having regular, or near-regular, triangles is two-fold: it

not only encourages edges to be of similar length (and thus have similar weighting in a line integration), but it also encourages shorter edges which reduces the two-dimensional scale on which the calculation will apply. It is important to note that while maximizing the minimum angle encourages shorter edges overall, a Delauney triangulation does not guarantee a minimization of triangle edge length (Lloyd 1977).

As mentioned previously, the polygon construction process begins with a Delauney triangle tessellation, an example of which is given in Fig. 1a. For each observation, the set of all other observations which share an edge, referred to as an observation's neighborhood, is located (Fig. 1b). The neighborhood polygon for an observation is defined by its neighborhood vertices, as depicted in Fig. 1c. The
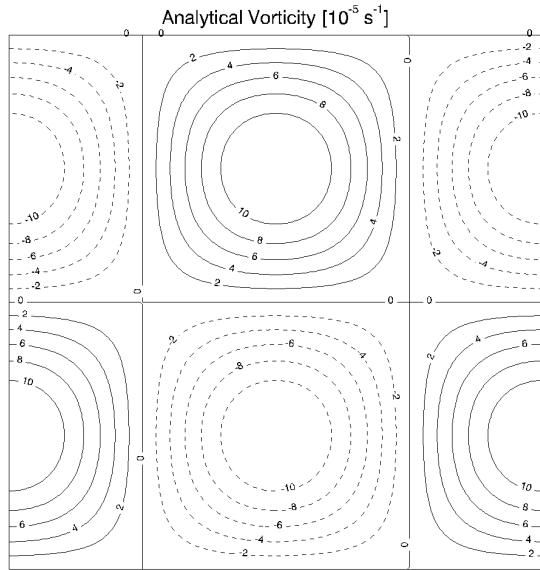
Fig. 2. Analytic vorticity on a 1000 km by 1000 km domain. Solid contours indicate positive vorticity while broken contours indicate negative vorticity.

Fig. 3. Example of a lawnmower-pattern flight path (red) with 30 randomly perturbed observations (asterisks) and corresponding Delauney triangle tessellation. Note the domain is 1000 km by 1000 km.

mean wind is then calculated for each edge (Fig. 1d) and decomposed (Fig. 1e) into its zonal and meridional components. Using the equations provided in Table 1 and repeating the process for each observation, a field of values can be calculated. An example of the calculated vorticity field is provided in Fig. 1f. It is worth noting that in instances where the observation lies on the outer edge of the tessellation, i.e. on the convex hull, the observation is used alongside its neighborhood vertices to reduce the frequency of triangular neighborhood polygons.

4. Evaluation of Accuracy

In order to evaluate the accuracy of the method proposed here, artificial observations are generated using sinusoidal variations in the meridional and zonal winds, as in Spencer and Doswell (2001), such that an analytical solution for the spatial derivatives is attainable. An example of the resulting analytic vorticity is shown in Fig. 2. As an in-depth comparison between using a Cartesian interpolation approach and a triangle-based line integration approach is provided by Spencer and Doswell (2001), this study limits the comparison to using polygonal and triangular regions in a line-integration approach. For brevity, only the accuracy of the vorticity is examined here.

Since the proposed method was developed in order to analyze vorticity from dropsonde wind observations, the error analysis provided here distributes the artificial observations along a number of flight paths. The observations
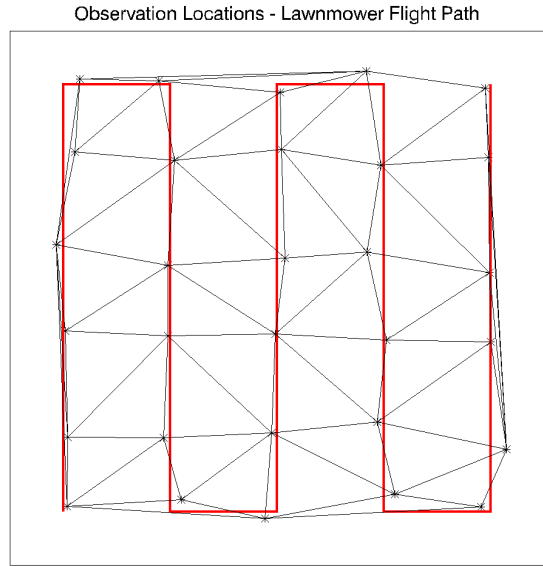
are positioned by first evenly distributing them along the flight path and then applying a random two-dimensional perturbation. The error analysis is limited to a lawnmower-pattern flight path here due to space constraints. An example of a lawnmower flight path is highlighted in red in Fig. 3. Also included in Fig. 3 are the observation locations (asterisks at the triangle vertices) as well as the corresponding Delauney triangle tessellation.

The vorticity fields which result from performing the line-integral method calculations on triangular and polygonal regions are depicted in Fig. 4a and Fig. 4b, respectively. Note the sharp gradients and extreme values present on the edges of the triangle-based analysis are not present in the polygon-based analysis. These values are caused by calculations on long, narrow triangles often found near the edge of the observation domain (see Fig. 3) which have relatively small areas and give overwhelming weight to the most distant observation. It is worth noting that, although most studies which rely on triangular regions remove these long, narrow triangles, the polygonal region approach retains the data that would otherwise be thrown out. Although the polygonal regions reduce the errors caused by these triangles (through reducing the influence of individual observations) caution should be exercised when sharp gradients are present. Also noteworthy is the difference in magnitude between the analytic vorticity (Fig. 2) and the calculated vorticities (Fig. 4). The primary drawback of

a)

Triangle Based Vorticity [10⁻⁵ s⁻¹] - Lawnmower Flight Path

b)

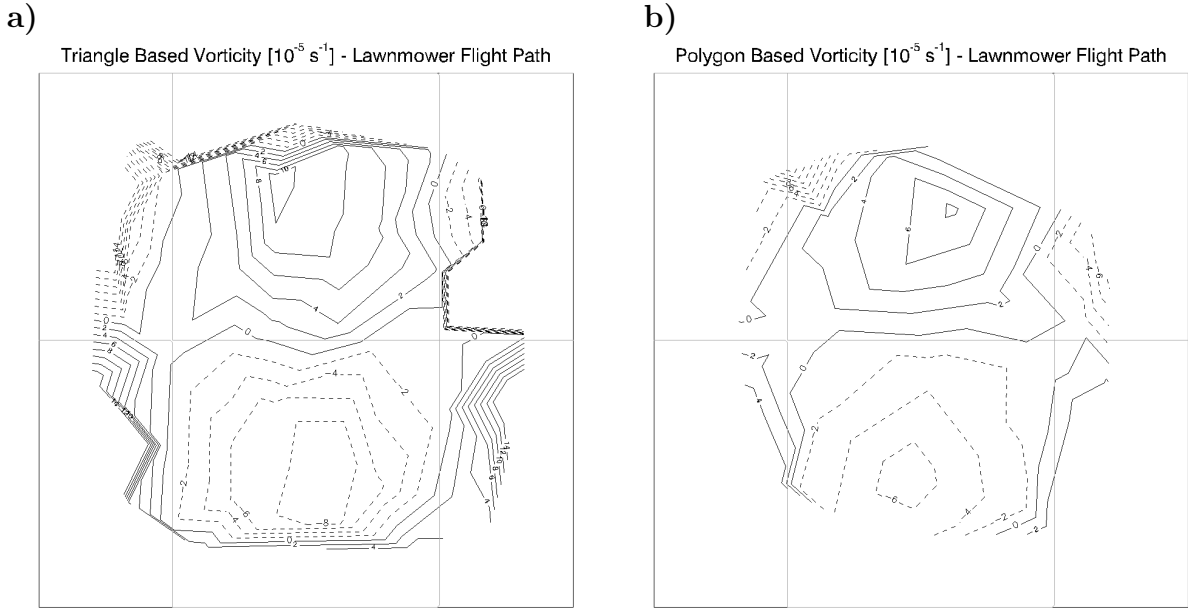Polygon Based Vorticity [10⁻⁵ s⁻¹] - Lawnmower Flight Path

FIG. 4. Vorticity field calculated using the line-integral method with (a) triangular regions and (b) polygonal regions on a 1000 km by 1000 km domain. The light gray horizontal and vertical lines indicate the analytic relative vorticity zero-lines (see Fig. 2) and are included for pattern comparison. The artificial observations are distributed as per Fig. 3.

a)

Lawnmower Flight Path RMSE - Full Domain
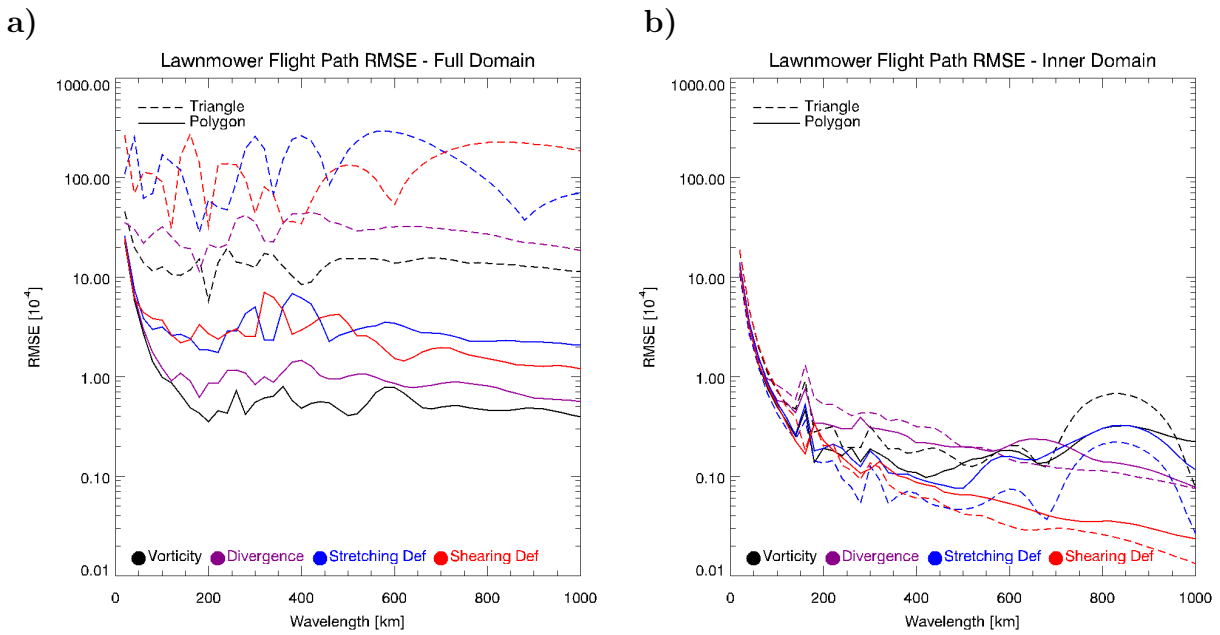
b)

Lawnmower Flight Path RMSE - Inner Domain

FIG. 5. Root-mean-square error calculated over (a) the full domain and (b) an inner domain which excludes the outer 250 km. Calculations are performed using 100 sets of 30 observations with randomly perturbed locations based on a lawnmower flight path. The error is calculated using the analytic fields (e.g. Fig. 2) as the base truth. Errors resulting from a triangle-based approach are plotted with a broken line and those resulting from a polygon-based approach are plotted with a solid line. Note that the wavelength corresponding to Fig. 2 is 1000 km. For reference, the RMSE of divergence (purple), stretching deformation (blue), and shearing deformation (red) are included in addition to the RMSE of vorticity (black).

4

using Green's Theorem for calculating spatial derivatives is that the extrema are muted, an effect which is more pronounced when polygonal regions are used.

The root-mean-square error (RMSE) is calculated over the entire domain (Fig. 5a) as well as over an inner domain which excludes the outer 250 km (Fig. 5b). Note the reduction in the full domain RMSE when using polygonal regions exceeds an order of magnitude for features with a wavelength greater than 150 km. As previously noted, this vast improvement results from an increased robustness to long, narrow triangles. By restricting the calculations to the inner domain, these triangles are excluded from the RMSE, resulting in far less of a difference in RMSE values.

5. Conclusions

A new line-integral method is proposed for calculating spatial derivatives from non-uniform observations. This method uses polygonal regions instead of the triangular regions used by previous studies. By using polygonal regions, the method is more robust to the long, narrow triangles which result in large errors in triangle-based calculations. While these error-prone triangles are usually removed from triangle-based analyses, the use of polygonal regions allows this data to be retained. Furthermore, when these triangles are not present, there is very little difference between polygon- and triangle-based methods in terms of RMSE. Finally, it is worth noting that this method can be used to calculate any spatial derivative and is not limited to those involving wind vectors. Additional examples of analyses using the proposed method are available in Helms and Hart (2012, 10A.2).

REFERENCES

Bourassa, M. A., and K. M. Ford, 2010: Uncertainty in scatterometer-derived vorticity. *J. Atmos. Oceanic Technol.*, **27**, 594–603.

Helms, C. N., and R. E. Hart, 2012: The evolution of dropsonde-derived vorticity in developing and non-developing tropical convective systems. *Extended Abstracts, 30th Conf. on Hurricanes and Tropical Meteorology*, Ponte Vedra, Florida, Amer. Meteor. Soc.

Lloyd, E. L., 1977: On triangulation of a set of points in the plane. Technical Report MIT/LCS/TM-88, Laboratory for Computer Science, Massachusetts Institute of Technology, 13 pp., Cambridge, Massachusetts.

Montgomery, M. T., and Coauthors, 2011: The predepression investigation of cloud systems in the tropics (PREDICT): Scientific basis, new analysis tools and some first results. *Bull. Amer. Meteor. Soc.*, **93**, 153–172.

Spencer, P. L., and C. A. Doswell, 2001: A quantitative comparison between traditional and line integral methods of derivative estimation. *Mon. Wea. Rev.*, **129**, 2538–2554.